www.czasopisma.pan.pl PAN www.journals.pan.pl
Chemical and Process Engineering 2020, 41 (2), 129–141
DOI: 10.24425/cpe.2020.132536

Adsorption of bisphenol a from aqueous solutions by activated tyre pyrolysis char – Effect of physical and chemical activation

Krzysztof Kuśmierek[1], Andrzej Świątkowski[1], Tomasz Kotkowski[2], Robert Cherbański[2,*], Eugeniusz Molga[2]

[1] Military University of Technology, Faculty of Advanced Technologies and Chemistry, ul. Kaliskiego 2, 00-908 Warsaw, Poland
[2] Warsaw University of Technology, Faculty of Chemical and Process Engineering, ul. Waryńskiego 1, 00-645 Warsaw, Poland

This paper aims to show the effect of activation method of tyre pyrolysis char (TPC) on adsorption of bisphenol A (BPA) from aqueous solutions. The TPC was produced from end-of-life-tyres (ELT) feedstock in a pilot plant at 773 K. Activation was accomplished using two classical methods: physical activation with CO_2 and chemical activation with KOH. The two produced adsorbents had pores ranging from micro- to macropores. Distinct differences in the BET surface areas and pore volumes between the adsorbents were displayed showing better performance of the chemically activated adsorbent for adsorption of BPA from water.

The results of the kinetic studies showed that the adsorption of BPA followed pseudo-second-order kinetic model. The Freundlich, Langmuir, Langmuir–Freundlich and Redlich–Peterson isotherm equations were used for description of the adsorption data. The Langmuir–Freundlich isotherm model best fits the experimental data for the BPA adsorption on both adsorbents. The Langmuir–Freundlich monolayer adsorption capacity, q_{mLF}, obtained for the CO_2-activated tyre pyrolysis char (AP-CO_2) and KOH-activated tyre pyrolysis char (AP-KOH) were 0.473 and 0.969 mmol g^{-1}, respectively.

Keywords: bisphenol A, adsorption, tyre pyrolysis char, physical activation, chemical activation

1. INTRODUCTION

Used tyres are categorised as part-worn tyres and end-of-life-tyres (ELTs). Whereas part-worn tyres can be treated in a few ways (e.g. exported or reused after rethreading), ELTs cannot be reused on vehicles anymore and should be reprocessed to decrease their negative environmental impact. According to the World Business Council for Sustainable Development, one passenger tire per person is discarded each year in the developed world and one billion ELTs are generated globally each year (World Business Council for Sustainable Development, 2008).

Even though ELTs are classified as non-hazardous waste (Council of the European Communities, 1991), direct disposal of ELTs in landfills is banned in the majority of developed countries. In the EU, this issue is regulated by Directive on the Landfill of Waste (Council of the European Communities, 1999). According

* Corresponding author, e-mail: Robert.Cherbanski@pw.edu.pl

to this directive, landfill of whole and shredded ELTs is prohibited. Instead, the following recovery routes of ELTs exist: material recovery and energy recovery. Material recovery is organized through various civil engineering applications (e.g. coastal protection, slope stabilization, road embankments, sound barriers) and recycling (e.g. pyrolysis, granulation, dock fenders). Within energy recovery, ELTs are used as supplementary fuel mainly in cement kilns.

Pyrolysis of ELTs involves the thermal decomposition of ELTs in the absence of air. The primary pyrolysis products are char (33%), oil (35%) gas (20%) and metal (12%) (Sharma et al., 1998). Given that the prices obtained for the primary pyrolysis products often do not justify the process costs, pyrolysis of ELTs is not a common method of material recovery. In the EU, only 12000 tonnes of ELTs were pyrolyzed compared to 1469000 tonnes that were granulated in 2017 (ETRMA, 2019). Therefore, to improve the process economic viability, the primary pyrolysis products should be valorized.

As far as tyre pyrolysis char (TPC) is concerned, such valorisation is connected with physical and chemical activation. Physical activation is carried out using CO_2 or steam. The reported BET surface areas are within wide ranges: between 250 and 1014 m^2/g for CO_2 activation, and between 272 and 1317 m^2/g for steam activation (Antoniou et al., 2014). With regard to chemical activation usually KOH is used. The reported BET surface areas are in the range between 242 and 981 m^2/g (Antoniou et al., 2014).

Activated tyre pyrolysis chars (ATPCs) have been successfully applied for purification of water from: different dyes (Acevedo et al., 2015; Daraei and Mittal, 2017; Shaid et al., 2019; Song et al., 2014), phenol (Helleur et al., 2001; Li et al., 2005; San Miguel, et al., 2002; San Miguel et al., 2003) and other organic compounds such as: 1,3-dichlorbenzene, 1,3-dinitrobenzene, 2,4-dichlorophenol (Lian et al., 2011), 2-chlorophenol (Manirajah et al., 2019), toluene (Zhu et al., 2011), metals ions as: Co(II), Cr(VI), Cu(II), Ni(II), Pb(II) (Abbasi et al., 2019; Makrigianni et al., 2017; Saleh et al., 2013), and rare earth elements (Smith et al., 2016).

Also, our previous works showed possible applications of CO_2-activated tyre pyrolysis char for removal of n-hexane from gas phase (Kotkowski et al., 2020), and phenol and chlorophenols (Kuśmierek et al., 2020a) as well as herbicides (Kuśmierek et al., 2020b) from aqueous solutions.

BPA is a chemical compound used in large scale in the production of thermal paper, synthetic polymers and epoxy resins and, in consequence, is present in many everyday products (Im and Löffler, 2016; Michałowicz, 2014). BPA is an endocrine disruptor that is toxic to humans as well as aquatic organisms. Water, including drinking water, is one of the major routes of BPA exposure. Due to the possible adverse health effects of BPA exposure its removal from water is a very important and current problem (Liang et al., 2015).

Based on the literature review, it can be concluded that adsorption is one of the most effective and popular method for its removal from water (Bhatnagar and Anastopoulos, 2017; Liang et al., 2015). In many studies, efficient, conventional and non-conventional adsorbents of BPA, including natural adsorbents, carbon and silica based adsorbents, composite materials and nanomaterials, agricultural wastes, were searched and experimentally checked (Antero et al., 2019; Bhatnagar and Anastopoulos, 2017; Heo et al., 2019; Juhola et al., 2020; Li et al., 2015; Ortiz-Martínez et al., 2016; Sudhakar et al., 2016; Wang and Zhang, 2020).

This work shows the potential of TPC upgrading by physical and chemical activation for the removal of BPA from aqueous solution. Unlike the previous work presenting the results of BPA adsorption on activated TPC (Acosta et al., 2018), the current work concerns the use of non-standardized TPC, which is produced in a pyrolysis pilot plant. A pyrolysis reactor in this pilot plant, having working volume of about 75 dm^3, is fed with 20 kg of ELTs of various types and brands.

2. MATERIALS AND METHODS

2.1. Reagents

Bisphenol A (BPA, CAS number 80057) with purity ≥ 98% was received from Sigma–Aldrich (St. Louis, USA). Potassium hydroxide (purity 85 wt %) was purchased from Chempur (Piekary Śląskie, Poland). All other chemicals were obtained from Avantor Performance Materials (Gliwice, Poland).

2.2. Preparation of activated tyre pyrolysis chars

A batch of 20 kg of ELTs was pyrolyzed at 773 K under nitrogen atmosphere to obtain TPC. The TPC, oil and gas yielded 39 wt %, 55 wt % and 6 wt %, respectively. The ELT feedstock consisted of shredded tyres of different types and brands without steel cords. Pyrolysis was carried out in a pilot plant, which was designed and built at the Faculty of Chemical and Process Engineering (Warsaw University of Technology, Poland). A detailed description of the pilot plant is presented elsewhere (Kuśmierek et al., 2020).

Physical activation of the TPC was accomplished in an electric tube furnace. Prior to activation, thermogravimetric analysis (TGA) was carried out to determine the optimal activation temperature and time (Kotkowski et al., 2018). Since heat transfer resistance can be usually neglected in TGA, unlike the activation of larger samples in the electric furnace, a few CO_2-activated tyre pyrolysis chars were fabricated in the electric furnace with increasing activation times, holding the optimal temperature. The sample with the highest BET surface area due to activation (255 m^2/g) was chosen for further tests. This sample was activated for 135 min with a flow rate of 0.5 dm^3/min at 1373 K under CO_2 atmosphere.

In general, many earlier experimental results show that the BET surface area increases with the increasing KOH/TPC mass ratio and reaches its maximum when the ratio is 4 (Antoniou et al., 2014; Marsh et al., 1984; Mui et al., 2004). Using this ratio, chars obtained from various materials were activated with KOH (Antoniou and Zabaniotou, 2015; Antoniou and Zabaniotou, 2018; Doczekalska et al., 2017; Gupta et al., 2011; Luo et al., 2016; Marsh et al., 1984; Teng et al., 2000). As a result, the same ratio was established in the present work.

Chemical activation was performed in the following steps (Gupta et al., 2011). Firstly, TPC was added to KOH at a mass ratio of 1:4. Secondly, the blend was mixed with a mortar for 10 minutes. Thirdly, 11.5 g of the blend was placed into the electric tube furnace. Fourthly, chemical activation was carried out at 1123 K for 90 min under a nitrogen atmosphere at a flow rate of 0.5 $dm^3\ min^{-1}$. When the mixture was cooled, it was neutralized by 0.02 M HCl and then flushed with distilled water. Finally, the activated tyre pyrolysis char (ATPC) was dried in an electric oven at 373 K for 60 min.

2.3. Adsorbent characterisation

The ATPCs were characterized by nitrogen adsorption/desorption isotherms at 77 K. The analyses were performed using a 3Flex Surface Characterization Analyser (Micromeretics, USA). The specific surface area was calculated from a BET plot in the appropriate pressure range determined according to the procedure proposed by Rouquerol (2007). The porosity parameters (micro- and mesopore volumes) were calculated according to procedures considered by Condon (2020).

2.4. Adsorption study

Batch adsorption experiments were conducted at laboratory scale using the bottle-point method. The equilibrium adsorption experiments were carried out by contacting in Erlenmeyer's flasks a constant

mass of adsorbent (0.02 g) with a 0.02 L of BPA solutions of initial concentrations ranging from 0.2 to 1.0 mmol L^{-1} (45.6 to 228 mg L^{-1}). The flasks were agitated at 25 °C at a constant speed (200 rpm) until equilibrium was reached.

The time-dependent adsorption experiments were carried out under the same conditions for initial BPA concentration of 0.5 mmol L^{-1} (114 mg L^{-1}). The adsorbate-adsorbent mixtures were agitated continuously and the samples were taken at different time intervals and analyzed for BPA concentration. The adsorption capacities of the adsorbents towards BPA at equilibrium (q_e) and at time t (q_t) were determined with the following equations:

$$q_t = \frac{(C_0 - C_t)V}{m} \tag{1}$$

$$q_e = \frac{(C_0 - C_e)V}{m} \tag{2}$$

All the adsorption experiments were carried out in duplicate, and average values were used for further calculations.

The concentration of BPA was measured using high-performance liquid chromatography with UV detection (Shimadzu LC-20, Kyoto, Japan). A Luna C-18, 4.6 × 150 mm, 3 μm column (Phenomenex, Torrance, USA) was used for all separations. The mobile phase, eluent flow-rate and detection wavelength were 55/45 (acetonitrile/water), 0.25 mL min^{-1} and 276 nm, respectively. The calibration curve was obtained by plotting peak height against the BPA concentration. With no outliers excluded (n = 3) the calibration curve was linear in the tested range from 0.01 to 0.5 mmol L^{-1} (0.228 to 114 mg L^{-1}) ($y = 2.945x + 0.115$, $R^2 = 0.999$).

3. RESULTS AND DISCUSSION

The porous structure of both obtained activated tyre pyrolysis chars was characterized on the basis of determined low temperature nitrogen adsorption/desorption isotherms (Fig. 1).

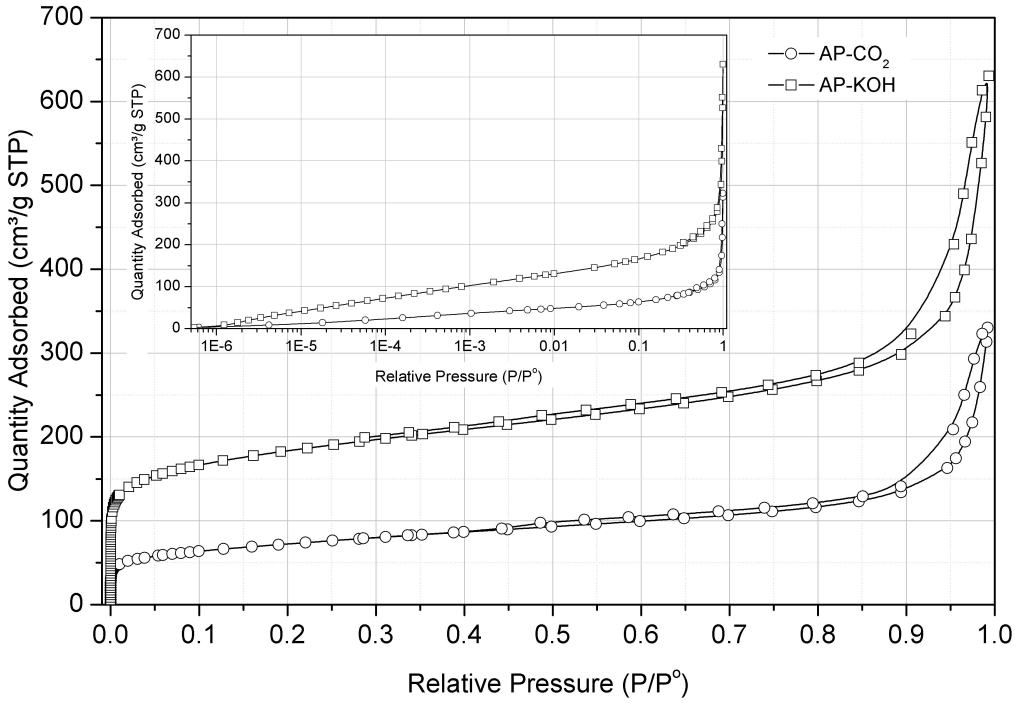

Fig. 1. Nitrogen adsorption-desorption isotherms at 77 K for activated tyre pyrolysis char AP-CO_2 and AP-KOH

The BET surface areas as well as the pore volumes of the carbonaceous materials are listed in Table 1. The calculated values of porosity parameters are significantly higher for tyre pyrolysis char activated using of KOH. For example, V_{mi} is higher by about 2.25-times for AP-KOH than AP-CO_2. In the case of V_{me} this ratio equals 1.8-times. To extend the porous structure characteristics, pore size distribution curves are plotted (Fig. 2).

Table 1. Porous structure of the activated tyre pyrolysis char

Adsorbent	S_{BET}, $m^2\ g^{-1}$	V_{mi}, $cm^3\ g^{-1}$	V_{me}, $cm^3\ g^{-1}$	$V_{mi}/(V_{mi} + V_{me})$
AP-CO_2	255	0.123	0.387	0.241
AP-KOH	667	0.278	0.693	0.286

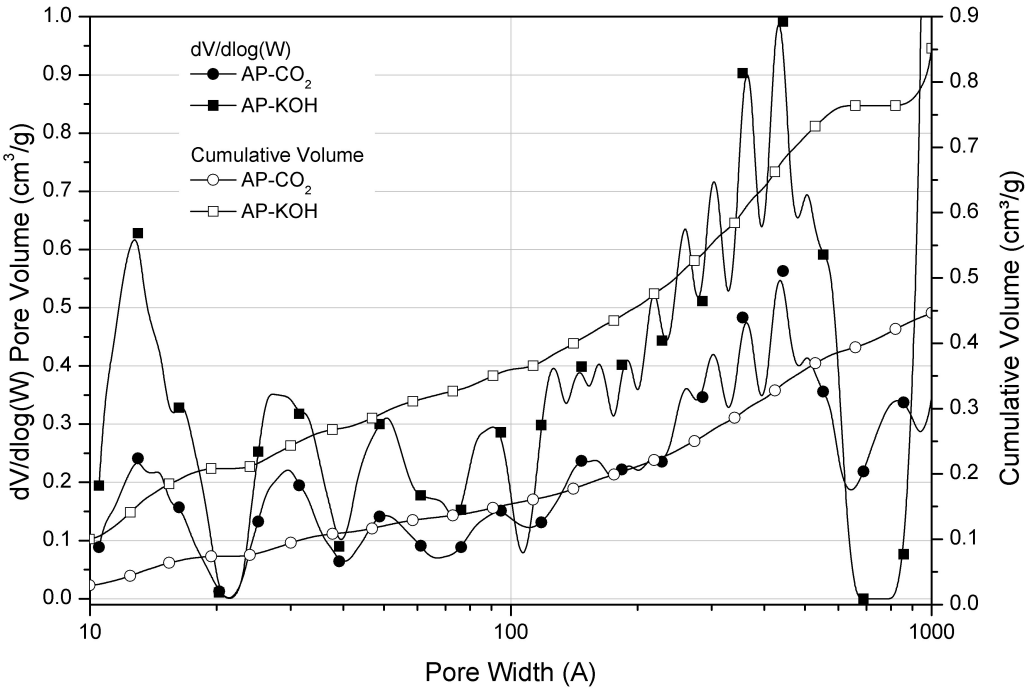

Fig. 2. Pore size distribution curves for activated tyre pyrolysis char AP-CO_2 and AP-KOH

The time profiles for the adsorption of BPA from water on the AP-CO_2 and AP-KOH materials are presented in Fig. 3. The adsorption capacity increased rapidly on both adsorbents in the first 60 min and then grew slowly till the adsorption equilibrium was achieved within about 120 min. The higher adsorption efficiency at the beginning of the process can be attributed to the higher availability of adsorption sites for the adsorbate molecules. As the contact time prolonged, the available adsorption sites diminished, resulting in a reduction in the uptake rate of the adsorbate.

The adsorption kinetic process was correlated with three kinetic models, namely, the pseudo-first-order (Eq. (3)), pseudo-second-order (Eq. (4)) and intra-particle diffusion (Eq. (5)):

$$\log(q_e - q_t) = \log q_e - \frac{k_1}{2.303}t \tag{3}$$

$$\frac{t}{q_t} = \frac{1}{k_2 q_e^2} + \frac{1}{q_e}t \tag{4}$$

$$q_t = k_i t^{0.5} + C_i \tag{5}$$

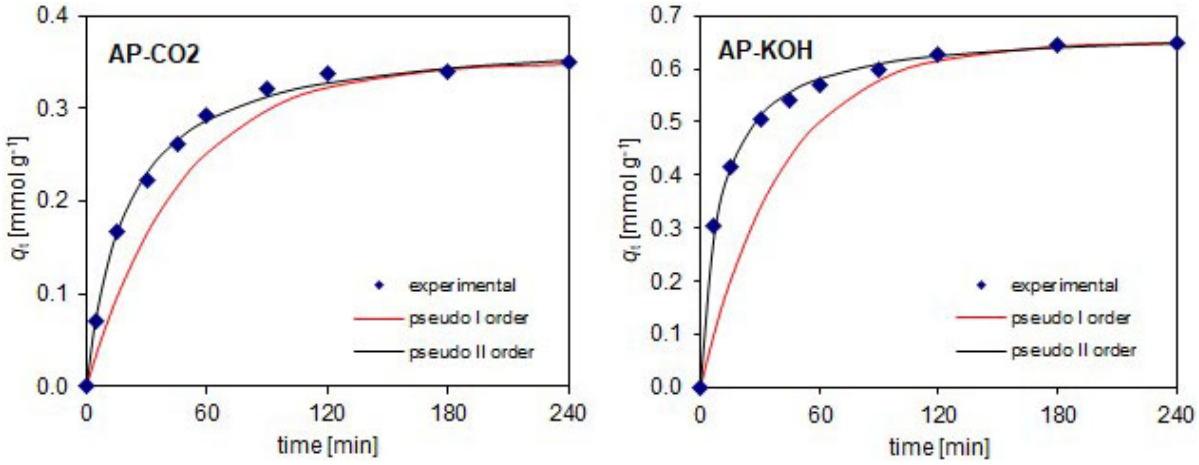

Fig. 3. Adsorption kinetics of BPA from water on the AP-CO_2 and AP-KOH activated tire pyrolysis chars (experimental conditions: C_0 = 0.5 mmol L^{-1} (114 mg L^{-1}), V = 0.02 L, m = 0.02 g)

The pseudo-first-order and pseudo-second-order kinetic parameters are summarized in Table 2. The values of k_1 and k_2 were calculated from the slope and intercept of the plots of $\log(q_e - q_t)$ vs. t and t/q_t vs. t, respectively.

Table 2. The pseudo-first-order and pseudo-second-order model constants for BPA adsorption on the AP-CO_2 and AP-KOH activated tire pyrolysis chars

Kinetic model	Adsorbent	
	AP-CO_2	AP-KOH
q_{exp}, mmol g^{-1}	0.351	0.652
pseudo-first-order model		
k_1, min^{-1}	0.0212	0.0244
q_{cal}, mmol g^{-1}	0.250	0.410
R^2	0.905	0.926
χ^2	0.0129	0.0177
pseudo-second-order model		
k_2, g·mmol^{-1}min^{-1}	0.134	0.154
q_{cal}, mmol g^{-1}	0.381	0.675
R^2	0.999	0.999
χ^2	0.0017	0.0033

The linear coefficients of R^2 determination and non-linear statistic Chi-square test (χ^2) were used to determine the model that best fitted the experimental data. The Chi-square test is expressed by Eq. (6):

$$\chi^2 = \sum_{i-1}^{n} \frac{(q_{exp} - q_{cal})^2}{q_{cal}} \tag{6}$$

As can be seen in Table 2, values of R^2 are equal to 0.999 for the pseudo-second-order kinetic model, which were much higher than the R^2 values obtained for the pseudo-first-order kinetic equation. The values of χ^2 obtained for the pseudo-second-order kinetic equation are lower than those observed for the pseudo-first-order. Furthermore, the experimental adsorption capacities q_{exp} are much closer to the calculated adsorption

capacities q_{cal} found from the pseudo-second-order kinetic model as compared to pseudo-first-order. This suggest that the adsorption of the BPA on both adsorbents follows the pseudo-second-order kinetic model.

The pseudo-second-order kinetic rate constants k_2 for adsorption of BPA on the AP-CO_2 and AP-KOH were 0.134 and 0.154 g·mmol^{-1}min^{-1}, respectively. So, BPA was adsorbed faster on the AP-KOH than on the AP-CO_2 activated tire pyrolysis char. This phenomenon can be explained by a higher mesopore volume of the AP-KOH (0.693 cm^3 g^{-1}) compared to the AP-CO_2 (0.387 cm^3 g^{-1}). It is well known that the porous structure of an adsorbent plays a crucial role in both adsorption kinetics and adsorption equilibria. Generally, a higher micropore volume (and thus a higher specific surface area) means greater adsorption efficiency (a higher adsorption capacity of an adsorbent), while a higher mesopore volume increases the rate of adsorption (Lorenc-Grabowska et al., 2014; Moreno-Castilla, 2004).

The intra-particle diffusion model, proposed by Weber and Morris (1963), was used to identify the mechanism involved in the adsorption process of the BPA. The plots of q_t versus $t^{0.5}$ for this model are shown in Fig. 4. As can be seen, the plots are non-linear over the whole time range and do not pass through the origin indicating that more than one process affected the adsorption and that the intra-particle diffusion was not the only rate-controlling step.

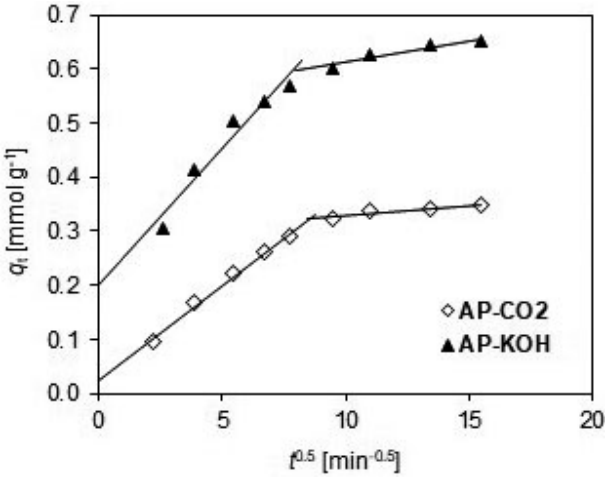

Fig. 4. Weber–Morris intra-particle diffusion models plots for BPA adsorption on the AP-CO_2 and AP-KOH activated tire pyrolysis chars (experimental conditions: C_0 = 0.5 mmol L^{-1} (114 mg L^{-1}), V = 0.02 L, m = 0.02 g)

Adsorption isotherms (Fig. 5) show the relationship between the amount of BPA adsorbed per unit mass of the adsorbent (q_e) versus the concentration of the adsorbate in the solution at equilibrium (C_e). The Freundlich (Eq. (7)), Langmuir (Eq. (8)), Langmuir–Freundlich (Eq. (9)) and Redlich–Peterson (Eq. (10)) isotherm equations were tested to fit the adsorption data:

$$q_e = K_F C_e^{1/n} \tag{7}$$

$$q_e = \frac{q_{mL} K_L C_e}{1 + K_L C_e} \tag{8}$$

$$q_e = \frac{q_{m\,LF}(K_{LF} C_e)^m}{1 + (K_{LF} C_e)^m} \tag{9}$$

$$q_e = \frac{A C_e}{1 + B C_e^{\beta}} \tag{10}$$

All model parameters were calculated with the non-linear least-squares method using OriginPro 8.0 software. The fitted adsorption isotherm models in this study are given in Fig. 5 while the relative parameters calculated from the four isotherm models are listed in Table 3.

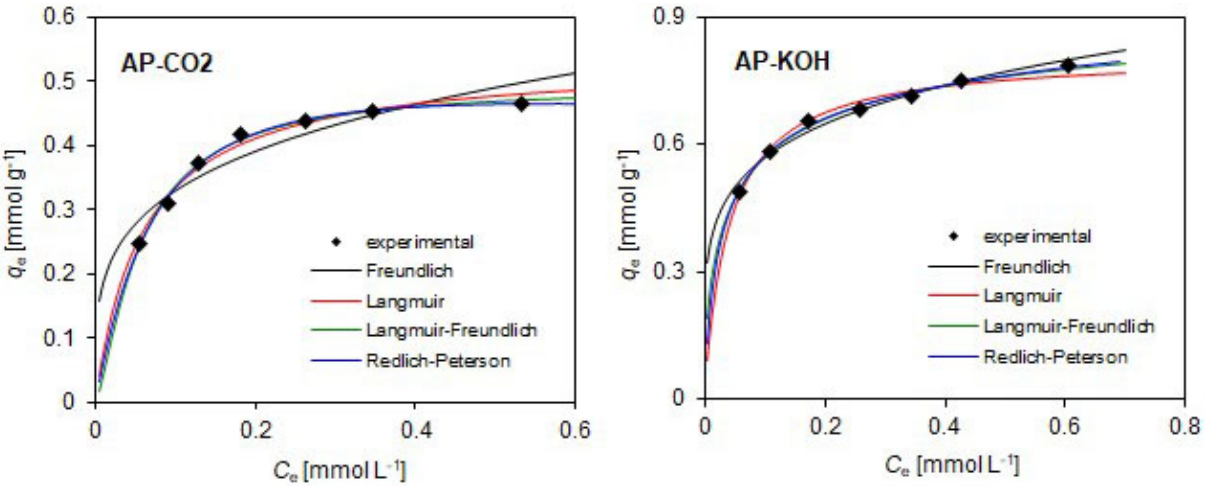

Fig. 5. Adsorption isotherms of BPA from water on the AP-CO_2 and AP-KOH activated tire pyrolysis chars

Table 3. Isotherm fitting parameters for BPA adsorption on the AP-CO_2 and AP-KOH activated tire pyrolysis chars

Isotherm model	Adsorbent	
	AP-CO_2	AP-KOH
Freundlich		
K_F [(mmol g^{-1})(L mmol^{-1})$^{1/n}$]	0.583	0.878
n	4.048	5.291
R^2	0.903	0.956
χ^2	0.00111	0.00029
Langmuir		
q_{mL} [mmol g^{-1}]	0.491	0.835
K_L[L mmol^{-1}]	16.72	24.19
R^2	0.983	0.978
χ^2	0.00014	0.00027
Langmuir–Freundlich		
q_{mLF} [mmol g^{-1}]	0.473	0.969
K_{LF}[L mmol^{-1}]	17.79	18.18
m	1.349	0.591
R^2	0.996	0.995
χ^2	0.00007	0.00010
Redlich–Peterson		
A [L g^{-1}]	6.621	14.89
B [L$^{\beta}$ mmol$^{-\beta}$]	13.49	20.93
β	0.939	0.904
R^2	0.973	0.979
χ^2	0.00014	0.00018

While analyzing the R^2 and χ^2 values of the isotherm models, the best fitting results for both the adsorbents were obtained with the Langmuir–Freundlich isotherm equation. In contrast, the Freundlich equation fitted the experimental data worst for the BPA adsorption as compared to the other three models due to the lowest correlation coefficient R^2 and highest χ^2 values. The Langmuir–Freundlich model is a combination of Langmuir and Freundlich isotherms which predicts the Langmuir model (monolayer adsorption) at high concentration of adsorbate and predicts the Freundlich model (multilayer adsorption) at low adsorbate concentration (Ayawei et al., 2017). The q_{mLF} values obtained for the AP-CO_2 and AP-KOH activated tire pyrolysis chars were 0.473 and 0.969 mmol g^{-1} (108 and 221 mg g^{-1}), respectively. The better BPA adsorption efficiency on the AP-KOH is correlated with its higher specific surface area (667 m^2 g^{-1}) compared to the AP-CO_2 (255 m^2 g^{-1}).

Table 4 compares the adsorption capacity of different types of adsorbents used for the removal of BPA from aqueous solutions.

Table 4. Comparison of BPA adsorption on various materials

Adsorbent	Adsorption capacity, mg g^{-1}	S_{BET}, m^2 g^{-1}	Ref.
Magnetic biochar	342	20.7	Wang and Zhang (2020)
$CuZnFe_2O_4$–biochar composite	263	61.5	Heo et al. (2019)
Activated charcoal	255	592	Zhao et al. (2019)
AP-KOH	221	667	this study
Waste coffee AC	123	1039	Alves et al. (2019)
KOH-activated TPC	123	700	Acosta et al. (2018)
AP-CO_2	108	255	this study
Multi-walled carbon nanotubes	95.1	182	Senin et al. (2018a)
Fullerene C60	74.0	4.26	Senin et al. (2018b)
Hydrodarco C commercial AC	73.1	485	Acosta et al. (2018)
Biomass-based carbon Fe-CR	41.5	103	Juhola et al. (2020)
Biomass-based carbon Fe-CR	23.8	74.0	Juhola et al. (2020)
Hydrothermal carbonizated AC-H2	21.3	441	Antero et al. (2019)
Tyre pyrolysis char (TCP)	17.1	350	Acosta et al. (2018)

4. CONCLUSIONS

A serious environmental problem associated with the generation of ELTs is being currently solved by two approaches – material and energy recovery. The ELT pyrolysis is considered only as an emerging method of material recovery. This is due to rather low profitability of the process. To improve its economics, valorization of pyrolysis products is required. As far as TPC is concerned, the viability of ELT pyrolysis can be enhanced by physical or chemical activation of TPC. In this paper, two activation methods are considered: (1) physical activation with CO_2 and (2) chemical activation with KOH. The two produced adsorbents (AP-CO_2 and AP-KOH) were used for the removal of BPA A from water. Distinct differences in the BET surface areas and pore volumes between the adsorbents showed better performance of the

chemical activation method. BPA was adsorbed faster and more efficiently on the AP-KOH than on the AP-CO_2, and the adsorption was closely correlated with the porous structure of the adsorbents used.

SYMBOLS

A	Redlich–Peterson isotherm constant, L g^{-1}
B	Redlich–Peterson isotherm constant, L^{β} $mmol^{-\beta}$
C_0	initial adsorbate concentration, mmol L^{-1}
C_e	final adsorbate concentration, mmol L^{-1}
C_i	thickness of the boundary layer
k_1	adsorption rate constant of the pseudo-first-order adsorption, min^{-1}
k_2	adsorption rate constant of the pseudo-second-order adsorption, g·$mmol^{-1}$$min^{-1}$
K_F	Freundlich isotherm constant, (mmol g^{-1})(L $mmol^{-1}$)$^{1/n}$
k_i	intra-particle diffusion rate constant, mmol g^{-1}·$min^{0.5}$
K_L	Langmuir isotherm constant related to the free energy of adsorption, L $mmol^{-1}$
K_{LF}	Langmuir–Freundlich constant representing the energy of adsorption, L $mmol^{-1}$
m	Langmuir–Freundlich empirical constant (dimensionless) or mass of adsorbent, g
n	Freundlich isotherm constants or number of replicated measurements
q_{cal}	adsorption capacity model-predicted value, mmol g^{-1}
q_e	adsorption capacity at equilibrium, mmol g^{-1}
q_{exp}	experimental adsorption capacity, mmol g^{-1}
q_{mL}	Langmuir maximum adsorption capacity, mmol g^{-1}
q_{mLF}	Langmuir–Freundlich monolayer adsorption capacity, mmol g^{-1}
q_t	adsorption capacity at time t, mmol g^{-1}
R^2	correlation coefficient
S_{BET}	specific surface area, m^2 g^{-1}
V	volume of the solution, L
V_{me}	mesopore volume, cm^3 g^{-1}
V_{mi}	micropore volume, cm^3 g^{-1}
V_t	total pore volume, cm^3 g^{-1}
β	Redlich–Peterson model exponent between 0 and 1
χ^2	statistic Chi-square test

REFERENCES

Abbasi S., Foroutan R., Esmaeili H., Esmaeilzadeh F., 2019. Preparation of activated carbon from worn tires for removal of Cu(II), Ni(II) and Co(II) ions from synthetic wastewater. *Desalin. Water Treat.,* 141, 269–278. DOI: 10.5004/dwt.2019.23569.

Acevedo B., Barriocanal C., Lupul I., Gryglewicz G., 2015. Properties and performance of mesoporous activated carbons from scrap tyres, bituminous wastes and coal. *Fuel*, 151, 83–90. DOI: 10.1016/j.fuel.2015.01.010.

Acosta R., Nabarlatz D., Sánchez-Sánchez A., Jagiello J., Gadonneix P., Celzard A., Fierro V., 2018. Adsorption of bisphenol A on KOH-activated tyre pyrolysis char. *J. Environ. Chem. Eng.*, 6, 823–833. DOI: 10.1016/j.jece.2018.01.002.

Alves A.C.F., Antero R.V.P., Oliveira S.B., Ojala S.A., Scalize P.S., 2019. Activated carbon produced from waste coffee grounds for an effective removal of bisphenol-A in aqueous medium. *Environ. Sci. Pollut. Res.*, 26, 24850–24862. DOI: 10.1007/s11356-019-05717-7.

Antero R.V.P., Alves A.C.F., Paulo Sales P.T.F., Oliveira S.B., Ojala S.A., Brum S.S., 2019. A new approach to obtain mesoporous-activated carbon via hydrothermal carbonization of Brazilian Cerrado biomass combined with physical activation for bisphenol – A removal. *Chem. Eng. Commun.*, 206, 1498–1514. DOI: 10.1080/00986445.2019.1601625.

Antoniou N., Stavropoulos G., Zabaniotou A., 2014. Activation of end of life tyres pyrolytic char for enhancing viability of pyrolysis – Critical review, analysis and recommendations for a hybrid dual system. *Renew. Sustain. Energy Rev.*, 39, 1053–1073. DOI: 10.1016/j.rser.2014.07.143.

Antoniou N., Zabaniotou A., 2015. Experimental proof of concept for a sustainable End of Life Tyres pyrolysis with energy and porous materials production. *J. Clean. Prod.*, 101, 1–14. DOI: 10.1016/j.jclepro.2015.03.101.

Antoniou N., Zabaniotou A., 2018. Re-designing a viable ELTs depolymerization in circular economy: Pyrolysis prototype demonstration at TRL 7, with energy optimization and carbonaceous materials production. *J. Clean. Prod.*, 174, 74–86. DOI: 10.1016/j.jclepro.2017.10.319.

Ayawei N., Ebelegi A.N., Wankasi D., 2017. Modelling and interpretation of adsorption isotherms. *J. Chem.*, 2017, Article ID 3039817. DOI: 10.1155/2017/3039817.

Bhatnagar A., Anastopoulos I., 2017. Adsorptive removal of bisphenol A (BPA) from aqueous solution: A review. *Chemosphere*, 168, 885–902. DOI: 10.1016/j.chemosphere.2016.10.121.

Condon J.B., 2020. *Surface area and porosity determinations by physisorption. Measurement, Classical theories and quantum theory*. Elsevier B.V., Amsterdam.

Council of the European Communities, 1991. Council Directive 91/156/EEC of 18 March 1991 amending Directive 75/442/EEC on Waste. Off. J. Eur. Communities L 078, 0032–0037.

Council of the European Communities, 1999. Council Directive 1999/31/EC of 26 April 1999 on the landfill of waste. Off. J. Eur. Communities L 182, 0001–0019.

Daraei H., Mittal A., 2017. Investigation of adsorption performance of activated carbon prepared from waste tire for the removal of methylene blue dye from wastewater. *Desalin. Water Treat.*, 90, 294–298. DOI:10.5004/dwt.2017.21344.

Doczekalska B., Pawlicka A., Kuśmierek K., Świątkowski A., Bartkowiak M., 2017. Adsorption of 4-chlorophenol from aqueous solution on activated carbons derived from hornbeam wood. *Wood Res.*, 62, 261–272.

ETRMA, 2019. ELT Management figures 2017.

Gupta V.K., Gupta B., Rastogi A., Agarwal S., Nayak A., 2011. Pesticides removal from waste water by activated carbon prepared from waste rubber tire. *Water Res.*, 45, 4047–4055. DOI: 10.1016/j.watres.2011.05.016.

Helleur R., Popovic N., Ikura M., Stanciulescu M., Liu D., 2001. Characterization and potential applications of pyrolytic char from ablative pyrolysis of used tires. *J. Anal. Appl. Pyrolysis*, 58–59, 813–824. DOI: 10.1016/S0165-2370(00)00207-2.

Heo J., Yoon Y., Lee G., Kim Y., Han J., Park C.M., 2019. Enhanced adsorption of bisphenol A and sulfamethoxazole by a novel magnetic CuZnFe2O4–biochar composite. *Bioresour. Technol.*, 281, 179–187. DOI: 10.1016/j.biortech.2019.02.091.

Im J., Löffler F.E., 2016. Fate of bisphenol A in terrestrial and aquatic environments. *Environ. Sci. Technol.*, 50, 8403–8416. DOI: 10.1021/acs.est.6b00877.

Juhola R., Runtti H., Kangas T., Hu T., Romar H., Tuomikoski S., 2020. Bisphenol A removal from water by biomass-based carbon: isotherms, kinetics and thermodynamics studies, *Environ. Technol.*, 41, 971–980. DOI: 10.1080/09593330.2018.1515990.

Kotkowski T., Cherbański R., Molga E., 2018. Acetone adsorption on CO_2-activated tyre pyrolysis char – Thermogravimetric analysis, *Chem. Process Eng.*, 39, 233–246. DOI: 10.24425/122946.

Kotkowski T., Cherbański, Molga E., 2020. Tyre-derived activated carbon – textural properties and modelling of adsorption equilibrium of n-hexane. *Chem. Process Eng.*, 41, 25–44. DOI: 10.24425/cpe.2019.130221.

Kuśmierek K., Świątkowski A., Kotkowski T., Cherbański R., Molga E., 2020a. Adsorption properties of activated tire pyrolysis chars for phenol and chlorophenols. *Chem. Eng. Technol.*, 43, 770–780. DOI: 10.1002/ceat.201900574.

Kuśmierek K., Świątkowski A., Kotkowski T., Cherbański R., Molga E., 2020b. Application of activated tire pyrolysis chars for the removal of selected herbicides from aqueous solutions. *Przem. Chem.*, 99 (6), 905–910. DOI: 10.15199/62.2020.6.15.

Li S.-Q.Q., Yao Q., Wen S.-E.E., Chi Y., Yan J.-H.H., 2005. Properties of pyrolytic chars and activated carbons derived from pilot-scale pyrolysis of used tires. *J. Air Waste Manage. Assoc.*, 55, 1315–1326. DOI: 10.1080/10473289.2005.10464728.

Li Y., Jin F., Wang C., Chen Y., Wang Q., Zhang W., Wang D., 2015. Modification of bentonite with cationic surfactant for the enhanced retention of bisphenol A from landfill leachate. *Environ. Sci. Pollut. Res.*, 22, 8618–8628. DOI: 10.1007/s11356-014-4068-0.

Lian F., Huang F., Chen W., Xing B., Zhu L., 2011. Sorption of apolar and polar organic contaminants by waste tire rubber and its chars in single- and bi-solute systems. *Environ. Pollut.*, 159, 850–857. DOI: 10.1016/j.envpol.2011.01.002.

Liang L., Zhang J., Feng P., Li C., Huang Y., Dong B., Li L., Guan X., 2015. Occurrence of bisphenol A in surface and drinking waters and its physicochemical removal technologies. *Front. Environ. Sci. Eng.*, 9, 1, 16–38. DOI: 10.1007/s11783-014-0697-2.

Lorenc-Grabowska E., Diez M.A., Gryglewicz G., 2016. Influence of pore size distribution on the adsorption of phenol on PET-based activated carbons. *J. Colloid Interf. Sci.*, 469, 205–212. DOI: 10.1016/j.jcis.2016.02.007.

Luo Y., Street J., Steele P., Entsminger E., Guda, V., 2016. Activated carbon derived from pyrolyzed pinewood char using elevated temperature, KOH, H_3PO_4, and H_2O_2. *BioResources*, 11, 10433-10447. DOI: 10.15376/biores.11.4.10433-10447.

Makrigianni V., Giannakas A., Bairamis F., Papadaki M., Konstaninou I., 2017. Adsorption of Cr(VI) from aqueous solutions by HNO_3-purified and chemically activated pyrolytic tire char. *J. Dispers. Sci. Technol.*, 38, 992–1002. DOI: 10.1080/01932691.2016.1216862.

Manirajah K., Sukumaran S.V., Abdullah N., Razak H.A., Ainirazali N., 2019. Evaluation of low cost-activated carbon produced from waste tyres pyrolysis for removal of 2-chlorophenol. *Bull. Chem. React. Eng. Catal.*, 14, 443–449. DOI: 10.9767/bcrec.14.2.3617.443-449.

Marsh H., Yan D.S., O'Grady T.M., Wennerberg A., 1984. Formation of active carbons from cokes using potassium hydroxide. *Carbon*, 22, 603–611. DOI: 10.1016/0008-6223(84)90096-4.

Michałowicz J., 2014. Bisphenol A – Sources, toxicity and biotransformation. *Environ. Toxicol. Pharmacol.*, 37, 738–758. DOI: 10.1016/j.etap.2014.02.003.

Moreno-Castilla C., 2004. Adsorption of organic molecules from aqueous solutions on carbon materials. *Carbon*, 42, 83–94. DOI: 10.1016/j.carbon.2003.09.022.

Mui E.L.K.K., Ko D.C.K.K., McKay G., 2004. Production of active carbons from waste tyres – A review. *Carbon*, 42, 2789–2805. DOI: 10.1016/j.carbon.2004.06.023.

Ortiz-Martínez K., Reddy P., Cabrera-Lafaurie W.A., Román F.R., Hernández-Maldonado A.J., 2016. Single and multi-component adsorptive removal of bisphenol A and 2,4-dichlorophenol from aqueous solutions with transition metal modified inorganicorganic pillared clay composites: effect of pH and presence of humic acid. *J. Hazard. Mater.*, 312, 262–271. DOI: 10.1016/j.jhazmat.2016.03.073.

Rouquerol J., Llewellyn P., Rouquerol F., 2007. Is the bet equation applicable to microporous adsorbents? *Stud. Surf. Sci. Catal.*, 160, 49–56. DOI: 10.1016/S0167-2991(07)80008-5.

Saleh T.A., Gupta V.K., Al-Saadi A.A., 2013. Adsorption of lead ions from aqueous solution using porous carbon derived from rubber tires: Experimental and computational study. *J. Colloid Interface Sci.*, 396, 264–269. DOI: 10.1016/j.jcis.2013.01.037.

San Miguel G., Fowler G.D., Sollars C.J., 2002. Adsorption of organic compounds from solution by activated carbons produced from waste tyre rubber. *Sep. Sci. Technol.*, 37, 663–676. DOI: 10.1081/SS-120001453.

San Miguel G., Fowler G.D., Sollars C.J., 2003. A study of the characteristics of activated carbons produced by steam and carbon dioxide activation of waste tyre rubber. *Carbon*, 41, 1009–1016. DOI: 10.1016/S0008-6223(02)00449-9.

Senin R.M., Ion I., Ion A.C., 2018a. A sorption study of bisphenol A in aqueous solutions on pristine and oxidized multi-walled carbon nanotubes. *Pol. J. Environ. Stud.*, 27, 2245–2257. DOI: 10.15244/pjoes/78677.

Senin R.M., Ion I., Oprea O., Vasile B., Stoica R., Ganea R., Ion A.C., 2018b. Sorption of bisphenol A (BPA) in aqueous solutions on fullerene C60. *Rev. Chim.*, 69, 1309–1314. DOI: 10.37358/RC.18.6.6316.

Shaid M.S.H.M., Zaini M.A.A., Nasri N.S., 2019. Isotherm, kinetics and thermodynamics of methylene blue dye adsorption onto CO_2-activated pyrolysis tyre powder. *Desalin. Water Treat.*, 143, 323–332. DOI: 10.5004/dwt.2019.23565.

Sharma V.K., Mincarini M., Fortuna F., Cognini F., Cornacchia G., 1998. Disposal of waste tyres for energy recovery and safe environment — Review. *Energy Convers. Manage.*, 39, 511–528. DOI: 10.1016/S0196-8904(97)00044-7.

Smith Y.R., Bhattacharyya D., Willhard T., Misra M., 2016. Adsorption of aqueous rare earth elements using carbon black derived from recycled tires. *Chem. Eng. J.*, 296, 102–111. DOI: 10.1016/j.cej.2016.03.082.

Song M., Tang M., Lv S., Wang X., Jin B., Zhong Z., Huang Y., 2014. The pyrolysis of multi-component municipal solid waste in fixed bed reactor for activated carbon production. *J. Anal. Appl. Pyrolysis*, 109, 278–282. DOI: 10.1016/j.jaap.2014.05.018.

Sudhakar P., Mall I.D., Srivastava V.C., 2016. Adsorptive removal of bisphenol-a by rice husk ash and granular activated carbon: a comparative study. *Desalin. Water Treat.*, 57, 12375–12384. DOI: 10.1080/19443994.2015.1050700.

Teng H., Lin Y.C., Hsu L.Y., 2000. Production of activated carbons from pyrolysis of waste tires impregnated with potassium hydroxide. *J. Air Waste Manag. Assoc.*, 50, 1940–1946. DOI: 10.1080/10473289.2000.10464221.

Wang J., Zhang M., 2020. Adsorption characteristics and mechanism of bisphenol A by magnetic biochar. *Int. J. Environ. Res. Public Health*, 17, 1075–1092. DOI: 10.3390/ijerph17031075.

Weber Jr. W., Morris J.C., 1963. Kinetics of adsorption on carbon from solution. *J. Sanit. Eng. Div.*, 18, 31–42.

World Business Council for Sustainable Development, 2008. *Managing end-of-life tires - Full report*. Available at: http://docs.wbcsd.org/2008/08/EndOfLifeTires-FullReport.pdf.

Zhao Y., Cho C.W., Cui L., Wei W., Cai J., Wu G., Yun Y.S., 2019. Adsorptive removal of endocrine-disrupting compounds and pharmaceutical using activated charcoal from aqueous solution: equilibrium, kinetics, and mechanism studies. *Environ. Sci. Pollut. Res.*, 26, 33897–33905. DOI: 10.1007/s11356-018-2617-7.

Zhu J., Liang H., Fang J., Zhu J., Shi B., 2011. Characterization of chlorinated tire-derived mesoporous activated carbon for adsorptive removal of toluene. *CLEAN – Soil, Air, Water*, 39, 557–565. DOI: 10.1002/clen.201000265.

Received 9 April 2020
Received in revised form 12 May 2020
Accepted 14 May 2020